

TE-dependent analysis of multi-echo fMRI with *tedana*

Elizabeth DuPre^{*1}, Taylor Salo^{†2}, Zaki Ahmed³, Peter A. Bandettini⁴, Katherine L. Bottenhorn², César Caballero-Gaudes⁵, Logan T. Dowdle⁶, Javier Gonzalez-Castillo⁴, Stephan Heunis⁷, Prantik Kundu⁸, Angela R. Laird², Ross Markello¹, Christopher J. Markiewicz⁹, Stefano Moia⁵, Isla Staden¹⁰, Joshua B. Teves⁴, Eneko Uruñuela⁵, Maryam Vaziri-Pashkam⁴, Kirstie Whitaker¹¹, and Daniel A. Handwerker^{‡4}

¹ McGill University ² Florida International University ³ Mayo Clinic ⁴ National Institutes of Health ⁵ Basque Center on Cognition, Brain and Language ⁶ Center for Magnetic Resonance Research, University of Minnesota ⁷ Eindhoven University of Technology ⁸ Mount Sinai Hospital ⁹ Stanford University ¹⁰ Thought Machine ¹¹ Alan Turing Institute

DOI: [10.21105/joss.03103](https://doi.org/10.21105/joss.03103)

Software

- [Review](#) ↗
- [Repository](#) ↗
- [Archive](#) ↗

Editor: [Pending Editor](#) ↗

Submitted: 09 March 2021

Published: 14 March 2021

License

Authors of papers retain copyright and release the work under a Creative Commons Attribution 4.0 International License ([CC BY 4.0](#)).

Summary

Functional magnetic resonance imaging (fMRI) is a popular method for in vivo neuroimaging. Modern fMRI sequences are often weighted towards the blood oxygen level dependent (BOLD) signal, which is closely linked to neuronal activity ([Logothetis, 2002](#)). This weighting is achieved by tuning several parameters to increase the BOLD-weighted signal contrast. One such parameter is “TE,” or echo time. TE is the amount of time elapsed between when protons are excited (the MRI signal source) and measured. Although the total measured signal magnitude decays with echo time, BOLD sensitivity increases ([Silvennoinen et al., 2003](#)). The optimal TE maximizes the BOLD signal weighting based on a number of factors, including several MRI scanner parameters (e.g., field strength), imaged tissue composition (e.g., grey vs. white matter), and proximity to air-tissue boundaries.

Even as optimal TE values vary by brain region, most whole-brain fMRI scans are “single-echo,” where signal is collected at a fixed TE everywhere in the brain. This TE value is often based on either a value that is best on average across all brain regions or an optimised value for a specific region of interest ([Peters et al., 2007](#); [Stöcker et al., 2006](#)). Generally, these choices reflect a tradeoff between BOLD weighting, overall signal-to-noise ratio (SNR), and signal loss due to magnetic susceptibility artifacts. Further, for any TE with BOLD signal there is also susceptibility to contamination from noise sources including head motion, respiration, and cardiac pulsation ([Caballero-Gaudes & Reynolds, 2017](#); [Chang & Glover, 2009](#); [Murphy et al., 2013](#); [Power et al., 2018](#)).

Rather than collect data at a single TE, an alternative approach is to collect multiple TEs (that is, multiple echos) for each time point. This approach, also known as multi-echo fMRI, has several benefits, including allowing researchers to estimate each voxel’s T_2^* value, combining echos ([Posse et al., 1999](#)), recovering signal in regions typically not sampled at longer echo times ([Kundu et al., 2013](#)), and improving activation and connectivity mapping ([Caballero-Gaudes et al., 2019](#); [Gonzalez-Castillo et al., 2016](#); [Lynch et al., 2020](#)) even in real time fMRI ([Heunis et al., 2020](#)). In addition, artifactual non- T_2^* changes (known as S_0 in this context) may be identified and removed by leveraging the relationship between BOLD contrast and T_2^* obtained with multi-echo fMRI ([Kundu et al., 2012](#)). Strategies to perform this efficiently and robustly are in active development.

^{*}co-first author

[†]co-first author

[‡]corresponding author

Continuing these efforts, we present *tedana* (TE-Dependent ANALysis) as an open-source Python package for processing and denoising multi-echo fMRI data. *tedana* implements two approaches to multi-echo preprocessing: (1) estimating a T_2^* map and using these values to generate a weighted sum of individual echos, and (2) using echo-time dependent information in analysis and denoising (Kundu et al., 2012).

We have tightly scoped *tedana* processing to focus on those portions of the fMRI analysis workflow which are multi-echo specific. The primary interfaces for users are (1) a *t2smap* workflow, which estimates voxel-wise T_2^* and S_0 and combines data across echos to increase temporal SNR, and (2) a full *tedana* workflow, which performs the same steps as the *t2smap* workflow and additionally performs ICA-based denoising to remove components exhibiting noise-like signal decay patterns across echos (Kundu et al., 2012). The *tedana* workflow additionally generates interactive HTML reports through which users may visually inspect their denoising results and evaluate each component's classification. An example report is presented in Figure 1.

Statement of Need

To date, multi-echo fMRI has not been widely adopted within the neuroimaging community. This is likely due to two constraints: (1) until recently, the lack of available multi-echo fMRI acquisition protocols, and (2) the lack of software for processing multi-echo fMRI data in a way that integrates with existing platforms, such as AFNI (Cox, 1996), SPM (Penny et al., 2011), FSL (Jenkinson et al., 2012), and fMRIPrep (Esteban et al., 2020).

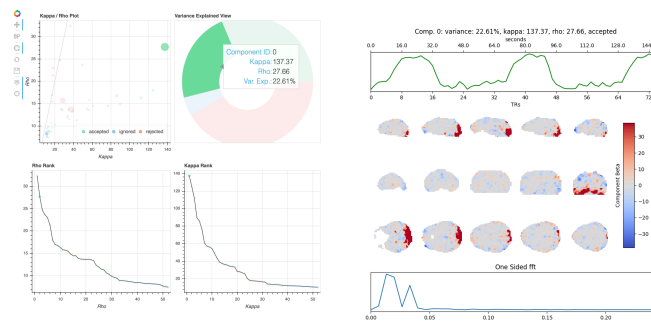
tedana helps to address these gaps both as a software tool and as a community of practice. As a software tool, its two use-case driven workflows each cover distinct, popular analyses in multi-echo fMRI processing. The limited focus and modularity of each workflow allows for easy integration into existing fMRI processing platforms. Individual modules also allow researchers to flexibly perform T_2^*/S_0 estimation, combination across echos, decomposition with PCA or ICA, and component selection outside of a specific workflow call. As a community of practice, *tedana* serves as a resource for researchers looking to learn more about multi-echo fMRI, from theory to collection to analysis. To specifically increase the availability of multi-echo protocols, *tedana*'s documentation (available at <https://tedana.readthedocs.io>) consolidates acquisition guidelines for multi-echo sequences across a variety of field strengths and scanner vendors, as well as general recommendations for balancing relevant trade-offs in fMRI acquisition parameter choices. It further serves to consolidate community knowledge, including guides explaining the underlying principles of multi-echo fMRI and information on publicly available multi-echo datasets and general recommendations for balancing relevant trade-offs in sequence development.

Although *tedana* is still in alpha release, it has already been incorporated into fMRIPrep and is supported by AFNI. *tedana* has additionally been used in a number of publications and conference presentations (Asyraf et al., 2020; Cohen et al., 2021; Lynch et al., 2020; Moia et al., 2020, 2021). We further hope that *tedana* will serve as a testing bed for new multi-echo related methods. To this end, we have developed a detailed contributing process and explicit project governance to encourage a healthy community and encourage other multi-echo research groups to contribute.

tedana is installable via PyPi (`pip install tedana`) and contains extensive documentation (<https://tedana.readthedocs.io>) to orient researchers to multi-echo fMRI acquisition and processing.

87 Figures

TEDANA 0.9.9-57.02/08F81 Reporting documentation



TE-dependence analysis was performed on input data.
An initial mask was generated from the first echo using Nilearn's `compute_epi_mask` function.
An adaptive mask was then generated, in which each voxel's value reflects the number of echoes with 'good' data.
A monoexponential model was fit to the data at each voxel using nonlinear model fitting in order to estimate T2* and S0 maps, using T2*/S0 estimates from a log-linear fit as initial values. For each voxel, the value from the adaptive mask was used to determine which echoes would be used to estimate T2* and S0. In cases of model fit failure, T2*/S0 estimates from the log-linear fit were retained instead.
Multi-echo data were then optimally combined using the T2* combination method (Posse et al., 1999).
Principal component analysis in which the number of components was determined based on a variance explained threshold was applied to the optimally combined data for dimensionality reduction.
A series of TE-dependence metrics were calculated for each component, including Kappa, Rho, and variance explained.
Independent component analysis was then used to decompose the dimensionally reduced dataset.
A series of TE-dependence metrics were calculated for each component, including Kappa, Rho, and variance explained.
Next, component selection was performed to identify BOLD (TE-dependent), non-BOLD (TE-independent), and uncertain (low-variance) components using the Kundu decision tree (v2.5; Kundu et al., 2013).
Rejected component time series were then orthogonalized with respect to accepted component time series.

Figure 1: An interactive report generated by *tedana*. Example reports can be accessed at: <https://me-ica.github.io/tedana-ohbm-2020/>

88 Acknowledgements

We would like to thank the Mozilla Open Leaders program, and the NIMH intramural research program, including the Section on Functional Imaging Methods and the Statistical and Scientific Computing Core, which have all provided funding or resources for *tedana* development.

Funding for ARL, KLB, and TS was provided by NIH R01-DA041353 and NIH U01-DA041156. Funding for KJW was provided through The Alan Turing Institute under the EPSRC grant EP/N510129/1.

95 References

- Asyraf, A., Lemarchand, R., Tamm, A., & Hoffman, P. (2020). Stimulus-independent neural coding of event semantics: Evidence from cross-sentence fMRI decoding. In *bioRxiv*. <https://doi.org/10.1101/2020.10.06.327817>
- Caballero-Gaudes, C., Moia, S., Panwar, P., Bandettini, P. A., & Gonzalez-Castillo, J. (2019). A deconvolution algorithm for multi-echo functional MRI: Multi-echo sparse paradigm free mapping. *Neuroimage*, 202, 116081. <https://doi.org/10.1016/j.neuroimage.2019.116081>
- Caballero-Gaudes, C., & Reynolds, R. C. (2017). Methods for cleaning the BOLD fMRI signal. *Neuroimage*, 154, 128–149. <https://doi.org/10.1016/j.neuroimage.2016.12.018>
- Chang, C., & Glover, G. H. (2009). Relationship between respiration, end-tidal CO₂, and BOLD signals in resting-state fMRI. *Neuroimage*, 47(4), 1381–1393. <https://doi.org/10.1016/j.neuroimage.2009.04.048>
- Cohen, A. D., Yang, B., Fernandez, B., Banerjee, S., & Wang, Y. (2021). Improved resting state functional connectivity sensitivity and reproducibility using a multiband multi-echo acquisition. *Neuroimage*, 225, 117461. <https://doi.org/10.1016/j.neuroimage.2020.117461>

- 110 Cox, R. W. (1996). AFNI: Software for analysis and visualization of functional magnetic
111 resonance neuroimages. *Computers and Biomedical Research*, 29(3), 162–173. <https://doi.org/10.1006/cbmr.1996.0014>
112
- 113 Esteban, O., Ciric, R., Finc, K., Blair, R. W., Markiewicz, C. J., Moodie, C. A., Kent, J. D.,
114 Goncalves, M., DuPre, E., Gomez, D. E. P., Ye, Z., Salo, T., Valabregue, R., Amlien, I.
115 K., Liem, F., Jacoby, N., Stojić, H., Cieslak, M., Urchs, S., ... Gorgolewski, K. J. (2020).
116 Analysis of task-based functional MRI data preprocessed with fMRIPrep. *Nature Protocols*,
117 15(7), 2186–2202. <https://doi.org/10.1038/s41596-020-0327-3>
- 118 Gonzalez-Castillo, J., Panwar, P., Buchanan, L. C., Caballero-Gaudes, C., Handwerker, D.
119 A., Jangraw, D. C., Zachariou, V., Inati, S., Roopchansingh, V., Derbyshire, J. A., &
120 Bandettini, P. A. (2016). Evaluation of multi-echo ICA denoising for task based fMRI
121 studies: Block designs, rapid event-related designs, and cardiac-gated fMRI. *Neuroimage*,
122 141, 452–468. <https://doi.org/10.1016/j.neuroimage.2016.07.049>
- 123 Heunis, S., Breeuwer, M., Caballero-Gaudes, C., Hellrung, L., Huijbers, W., Jansen, J. F.,
124 Lamerichs, R., Zinger, S., & Aldenkamp, A. P. (2020). The effects of multi-echo fMRI
125 combination and rapid T2*-mapping on offline and real-time BOLD sensitivity. In *bioRxiv*.
126 <https://doi.org/10.1101/2020.12.08.416768>
- 127 Jenkinson, M., Beckmann, C. F., Behrens, T. E. J., Woolrich, M. W., & Smith, S. M. (2012).
128 FSL. *Neuroimage*, 62(2), 782–790. <https://doi.org/10.1016/j.neuroimage.2011.09.015>
- 129 Kundu, P., Brenowitz, N. D., Voon, V., Worbe, Y., Vértes, P. E., Inati, S. J., Saad, Z. S.,
130 Bandettini, P. A., & Bullmore, E. T. (2013). Integrated strategy for improving functional
131 connectivity mapping using multiecho fMRI. *Proceedings of the National Academy of*
132 *Sciences of the United States of America*, 110(40), 16187–16192. <https://doi.org/10.1073/pnas.1301725110>
133
- 134 Kundu, P., Inati, S. J., Evans, J. W., Luh, W.-M., & Bandettini, P. A. (2012). Differentiating
135 BOLD and non-BOLD signals in fMRI time series using multi-echo EPI. *Neuroimage*,
136 60(3), 1759–1770. <https://doi.org/10.1016/j.neuroimage.2011.12.028>
- 137 Logothetis, N. K. (2002). The neural basis of the blood–oxygen–level–dependent functional
138 magnetic resonance imaging signal. *Philosophical Transactions of the Royal Society B:*
139 *Biological Sciences*, 357(1424), 1003–1037. <https://doi.org/10.1098/rstb.2002.1114>
- 140 Lynch, C. J., Power, J. D., Scult, M. A., Dubin, M., Gunning, F. M., & Liston, C. (2020).
141 Rapid precision functional mapping of individuals using Multi-Echo fMRI. *Cell Reports*,
142 33(12), 108540. <https://doi.org/10.1016/j.celrep.2020.108540>
- 143 Moia, S., Stickland, R. C., Ayyagari, A., Termenon, M., Caballero-Gaudes, C., & Bright, M. G.
144 (2020). Voxelwise optimization of hemodynamic lags to improve regional CVR estimates
145 in breath-hold fMRI. *Conference Proceedings - IEEE Engineering in Medicine and Biology*
146 *Society, 2020*, 1489–1492. <https://doi.org/10.1109/EMBC44109.2020.9176225>
- 147 Moia, S., Termenon, M., Uruñuela, E., Chen, G., Stickland, R. C., Bright, M. G., & Caballero-
148 Gaudes, C. (2021). ICA-based denoising strategies in Breath-Hold induced cerebrovascular
149 reactivity mapping with multi echo BOLD fMRI. *NeuroImage*, 117914. <https://doi.org/10.1016/j.neuroimage.2021.117914>
150
- 151 Murphy, K., Birn, R. M., & Bandettini, P. A. (2013). Resting-state fMRI confounds and
152 cleanup. *Neuroimage*, 80, 349–359. <https://doi.org/10.1016/j.neuroimage.2013.04.001>
- 153 Penny, W. D., Friston, K. J., Ashburner, J. T., Kiebel, S. J., & Nichols, T. E. (2011).
154 *Statistical parametric mapping: The analysis of functional brain images*. Elsevier.
155 ISBN: 9780123725608
- 156 Peters, A. M., Brookes, M. J., Hoogenraad, F. G., Gowland, P. A., Francis, S. T., Morris, P.
157 G., & Bowtell, R. (2007). T2* measurements in human brain at 1.5, 3 and 7 T. *Magnetic*
158 *Resonance Imaging*, 25(6), 748–753. <https://doi.org/10.1016/j.mri.2007.02.014>

- 159 Posse, S., Wiese, S., Gembris, D., Mathiak, K., Kessler, C., Grosse-Ruyken, M. L., Elghah-
160 wagi, B., Richards, T., Dager, S. R., & Kiselev, V. G. (1999). Enhancement of BOLD-
161 contrast sensitivity by single-shot multi-echo functional MR imaging. *Magnetic Reso-*
162 *nance in Medicine*, 42(1), 87–97. [https://doi.org/10.1002/\(sici\)1522-2594\(199907\)42:](https://doi.org/10.1002/(sici)1522-2594(199907)42:1%3C87::aid-mrm13%3E3.0.co;2-o)
163 [1%3C87::aid-mrm13%3E3.0.co;2-o](https://doi.org/10.1002/(sici)1522-2594(199907)42:1%3C87::aid-mrm13%3E3.0.co;2-o)
- 164 Power, J. D., Plitt, M., Gotts, S. J., Kundu, P., Voon, V., Bandettini, P. A., & Martin, A.
165 (2018). Ridding fMRI data of motion-related influences: Removal of signals with distinct
166 spatial and physical bases in multiecho data. *Proceedings of the National Academy of*
167 *Sciences of the United States of America*, 115(9), E2105–E2114. [https://doi.org/10.](https://doi.org/10.1073/pnas.1720985115)
168 [1073/pnas.1720985115](https://doi.org/10.1073/pnas.1720985115)
- 169 Silvennoinen, M. J., Clingman, C. S., Golay, X., Kauppinen, R. A., & Zijl, P. C. M. van.
170 (2003). Comparison of the dependence of blood R2 and R2* on oxygen saturation at 1.5
171 and 4.7 tesla. *Magnetic Resonance in Medicine*, 49(1), 47–60. [https://doi.org/10.1002/](https://doi.org/10.1002/mrm.10355)
172 [mrm.10355](https://doi.org/10.1002/mrm.10355)
- 173 Stöcker, T., Kellermann, T., Schneider, F., Habel, U., Amunts, K., Pieperhoff, P., Zilles, K.,
174 & Shah, N. J. (2006). Dependence of amygdala activation on echo time: Results from
175 olfactory fMRI experiments. *Neuroimage*, 30(1), 151–159. [https://doi.org/10.1016/j.](https://doi.org/10.1016/j.neuroimage.2005.09.050)
176 [neuroimage.2005.09.050](https://doi.org/10.1016/j.neuroimage.2005.09.050)

DRAFT